Supporting Information

The dynamic invertible intramolecular charge-transfer fluorescence probe: Real-time monitoring of mitochondrial ATPase activity

Hua Zhang,[a, b]* Yafu Wang,[a] Xiaopeng Xuan,[a] Ge Wang,[c] Haiming Guo,[a] Jiangli Fan[b,] *

[a] Collaborative Innovation Center of Henan Province for Green Manufacturing of Fine Chemicals, Key Laboratory of Green Chemical Media and Reactions, Ministry of Education Henan Key Laboratory of Green Chemical Media and Reactions, School of Chemistry and Chemical Engineering, Henan Normal University, 46 Jianshe Road, Muye Zone, Xinxiang 453007, P. R. China;

[b] State Key Laboratory of Fine Chemicals, School of Pharmaceutical Science and Technology, Dalian University of Technology, Dalian 116024, P.R. China;

[c] Xinxiang Medical University, 601 Jinsui Road, Hongqi Zone, Xinxiang 453000, P.R. China;

Corresponding Author Email: zhanghua1106@163.com, fanjl@dlut.edu.cn

Tel/Fax: +86-373-3329030.

Contents

1. Procedures section

A.R. grade of solvents and reagents were used in this work. Column chromatographic was used to purify compounds and silica gel (200-300 mesh) was used as fillers. Commercial fluorescent dye, MitoTracker Green FM was purchased from Life Technologies Co. (USA). ATPases (Enzyme Commission (EC) Number 3.6.1.3) was obtained from Sigma Chemical Co. (USA). Doubly purified water was used in all experiments, which was prepared using by a Milli-Q system. OPM and OPD- as stock were used in spectrographic determination and cell experiments. HPLC(Agilent 1290 Infinity)-HRMS (Bruker microToF II, Bruker Co., Switzerland) with an auto sampler operated in-line with a quantum triple quadrupole instrument was carried out in mass spectral studies on ESI positive or negative ion mode. NMR spectra were obtained from Avance 400 and 600 MHz spectrometer (Bruker Co., Switzerland). Isothermal titration calorimetry (ITC) was used NANO ITC Isothermal Titration Calorimeter.

Spectrographic determination in vitro.

A Lambd 950 spectrophotometer from PerkinElmer (USA) and a LS-55 spectrophotometer from PerkinElmer (USA) were used to measure absorption spectra and fluorescence spectra, respectively. In all spectral experiments, the final solutions contained < 5 ‰ DMSO. Each experiment was carried out in five replicates (n = 5). The relative fluorescence quantum yields were determined using Rhodamine B (ΦF = 0.97 in methanol) by the following equation:

$$\Phi_x = \Phi_s(F_x/F_s)(A_s/A_x)(\lambda_{exs}/\lambda_{exx})(n_x/n_s)^2 \quad (1)$$

where Φ represents quantum yield; F is the integrated area under the corrected emission spectrum; A is absorbance at the excitation wavelength; λex is the excitation wavelength; n is the refractive index of the solution (because of the low concentrations of the solutions, 10-7-10-8 mol/L, the refractive indices of the solutions were replaced with those of the solvents); and the subscripts x and s refer to the unknown and the standard, respectively. The detection limit was calculated by three times the standard deviation divided by the slope of the blank. The data were obtained from replicate experiments (n = 5)

Energy Measurement by ITC.

Follow these steps to prepare the solutions:

1. Prepare a large amount of buffer as appropriate for the experiment (add the appropriate type & amount of salts). This buffer will be used as material for formulation of the titrant solutions, and in their dialysis.
2. Formulate solutions of any large-molecule sample compounds at this time using the buffer solution. (Small-molecule sample compounds will be made up in a following step).
3. Dialyze the solution(s) inside the remaining buffer. Place the sample in a dialysis bag and suspend it inside the buffer solution. Gently stir the buffer for several hours to aid in the equalization of pH and the concentrations of electrolytes. Temperature-sensitive samples may need to remain chilled during this process.
4. Small molecule samples are prepared at this time using the dialyzed buffer. Not be dialyzed this solution.
5. Retain 50-300 mL of the dialyzed buffer for use later in cell rinsing and for optional blank experiments.

All solvents must be degassed prior to being placed in the ITC to minimize the possibility of gas bubble formation during the run. Pull a vacuum of 0.3-0.5 atm on the solutions for a period of 10-15 min to degas a sample.

Follow the instructions below to prepare the sample cells:

1. Use the filling syringe (shown in the figure to the right), to flush the sample cell several times with the same buffer solution in which the sample is prepared.

2. After flushing, remove all of buffer and slowly load the sample into the sample cell (middle access tube) inside the Nano ITC to allow air bubbles to evacuate through the top of the cell.

a. When liquid is just visible at the opening of the access tube, continue to gently inject, while slowly withdrawing it from the cell. This will maintain the fill level and prevent new bubbles from being introduced into the cell (see the figure to the right). When using aqueous solutions, the reference cell (side access tube) should be filled with water.

b. Make sure that the reference needle is inserted into the reference cell access tube after filling (see the figure on the next page). The liquid should be just visible at the bottom of the conical overflow reservoir when the cell is filled.

3. Load the 100 μL syringe with the titrant taking care to remove any bubbles from the barrel of the syringe, but leaving a small, 5 to 10 μL, air gap between the plunger tip and the liquid in the barrel. Leaving an air gap is a critical step, needed to prevent signal distortion. Fill the syringe to a slight excess, 2 or 3 mm beyond the highest gradation of the barrel.

4. Insert the plunger and barrel carefully into the rotating shaft of the burette assembly. (See the upper right figure).

5. Hold the rotating shaft on the burette securely in one hand. Use the knurled knob at the base of the syringe barrel to finger-tighten the syringe into place with the other hand. A small droplet will appear at the tip of the syringe. A small droplet will appear at the tip of the syringe.

6. Wipe any excess titrant from the needle along the exterior of the barrel and the tip.

7. Guide the shaft carefully, needle first, and into the top opening of the calorimeter (see the figure to the right). Make sure the key slots line up with the three locking posts located in the mounting ring at the top.

8. Gently push the burette handle downward and rotate it slightly clockwise to secure the burette in place.

9. Turn on the stirrer at 250 to 400 rpm.

10. Allow the system to re-equilibrate until the calorimeter heat reading is stable. See the NOTE in the left-hand column.

11. Set up the parameters for the particular experiment of interest using the ITC Run program under the Setup tab (see the online help for details).

12. Wait until a stable baseline is evident. (See the online help for details regarding baselines.) Then click on Experiment/Start or click the Go icon at the top of the toolbar to start the experiment.

13. Enter a filename when prompted. The program indicator on the Setup tab will be red when the program is active. You will be able to watch the progress of the experiment under the Monitor tab or the Data tab.

14. The titration data is automatically saved to disk at the conclusion of the experiment.

15. Evaluate the data using the Nano-Analyze software package. (See the online help for information.)

Mitochondrial ATPase is one of the enzymes associated with the energy metabolism. In other words, the change of mitochondrial ATPase activity can indicate the intracellular energy change. Thus, the energy changes were simultaneously detected by isothermal titration calorimetry (ITC, a standard method for detecting energy changes in live cells; Fig. 6a: 3.06 ± 0.21 cal., Fig. 6b: 2.12 ±0.17cal.) during this process. These results indicated that the energy decreased during apoptosis in cancer cells, which is consistent with that in reported work.[30,31]

Quantum Calculations.

Gaussian 09 was used in the entire quantum chemical. The density functional theory (DFT) with B3LYP functional was used in the geometry optimizations of the dyes. 6-311G (d, p) basis set was used. The electronic transition energies and corresponding oscillator strengths were calculated by time-dependent density functional theory (TD-DFT) at the B3LYP/6-311G (d, p) level. The water as a solvent was added into the quantum calculation.

Photostability in solution.

OPM and OPD- were dissolved in DMSO-water (5:5 v/v) all at concentrations of 5.0 μM. The solutions were irradiated by a 500W iodine-tungsten lamp situated 250 mm away for 7 h. An aqueous solution of sodium nitrite (50 g/L) was placed between the samples and the lamp as a light filter (to cut off the light shorter than 400 nm) and as a heat filter. The photostabilities were expressed in terms of remaining absorption (%) calculated from the changes of absorbance at the absorption maximum before and after irradiation by iodine-tungsten lamp. The absorbance was determined. The data were obtained from replicate experiments (n = 5).

Photostability in cells.

The fluorescence intensity was determined, after cell staining with 5.0 μM OPM and OPD- for 30 min at 37 ℃ under 5% CO2, by spectral confocal multiphoton microscopy (Olympus, FV1200) with a high-performance mode-locked titanium-sapphire laser source (MaiTai, Spectra-Physics, USA). The change of fluorescence intensity with scan time was determined by spectral confocal multiphoton microscopy (Olympus, FV1200) in the consecutive t-scan mode for 60 min. The intensity of OPM and OPD- were recorded with the relevant emission. Excitation wavelength: 800 nm with constant intensity. The data were obtained from replicate experiments (n=5).

Cell Culture.

Hepg 2 cell lines, RH35 cells lines, NIH 3T3 cell lines and CHO cell lines were obtained from the Chinese Academy of Medical Sciences. The red-free Dulbecco's Modified Eagle's Medium (DMEM, WelGene) and eagle's minimum essential medium (MEM, WelGene) supplemented with penicillin/streptomycin and 10 % fetal bovine serum (FBS; Gibco) were used for culture cells in a CO2 incubator at 37 ℃. One day before imaging, the cells mentioned above were seeded into confocal dishes with well glass bottom (MatTek, 1# glass, 0.13-0.16 mm). They were incubated at 37 ℃ in 5.0 wt %/vol CO2 for 24 h. And then, the cells were incubated with OPM at a certain concentration.

Fluorescence Imaging in Cells.

Olympus spectral confocal multiphoton microscope (FV1200) with MaiTai femtosecond laser source (Spectra-Physics) was used in image experiment. Inverted microscope was used in cell imaging. The imaging parameters are as follow. Internal PMTs = 16 bit, pixels = 1600 × 1600. Lasers: 800 nm, 515 nm and 559 nm. The scan ranges were ascertained according to fluorescence of dye.

Colocalization Imaging.

MitoTracker Green FM was used as standard dye for mitochondria. The cells were incubated with MitoTracker and OPM for 30 min under 5.0 wt % /vol CO2 at 37 ℃. After then, they were washed with PBS three times. And the cells were imaged in 1600 × 1600 pixels. The fluorescence imaging was analyzed by colocalization coefficient.

Dynamic Imaging.

Olympus spectral confocal multiphoton microscope (FV1200) with MaiTai femtosecond laser source (Spectra-Physics) was used in image experiment. Inverted microscope was used in cell imaging. Time scan mode was used. Internal PMTs = 16 bit, pixels = 1600 × 1600. Lasers: 800 nm. Time interval = 1.0 s.

Cytotoxicity.

Hepg 2 cell lines, RH35 cells lines, NIH 3T3 cell lines and CHO cell lines were prepared for cell viability studies in 96-well plates (1 × 105 cells per well that were incubated in 100 μL). The cells were incubated for an additional 24 h with dyes OPM in different concentrations. Subsequently, 100 μL of 3-(4,5-dimethylthiazol-2-yl)-2,5-diphenyltetrazolium bromide (MTT, Sigma Chemical Co. U.S.A.) was added into each well, followed by further incubation for 24 h at 37 °C. The DMEM was remove and DMSO (200 μL/well) added to dissolve the reddish-blue crystals. Optical density (OD) was determined by a microplate reader (Spectra Max M5, Molecular Devices) at 570

nm with subtraction of the absorbance of the cell-free blank volume at 630 nm. The results from the six individual experiments were averaged. The relative cell viability (100%) was calculated using the following equation:

$$\text{cell viability}(\%) = (\text{ODdye-ODk-dye})/(\text{ODctrl-ODk-ctrl}) \times 100 \quad (2)$$

Partition Coefficients.

The logarithms of the water/octanol partition coefficients (log Poct values) of OPM and OPD- were estimated using the computational procedure of Hansch and Leo. This procedure was used as it permits calculation of the log Poct values, as was required to discuss permeability, and also for use with the QSAR models. Log Poct estimations using the software available at this time do not provide values for ions, but only for the related nonionic bases.

2. Synthetic route of OPM

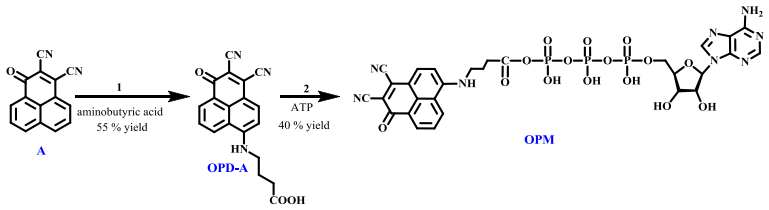

Scheme S1. The synthetic route of OPM and its optimized configuretion.

3. Synthetic procedures of OPM and intermediates

The synthesis of A (1-Oxo-1*H*-phenalene-2, 3-dicarbonitrile)

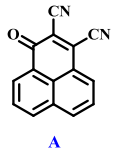

Synthesis of **A** was synthesized by the previously reported method [S1]. 2-(2-oxoacenaphthylen-1(2H)-ylidene)malononitrile (2.17 mmol, 500 mg) was suspended in anhydrous CH_3CN (40 mL). Under stirring, the mixture was heated to refluxed temperature and then added the base. After complete consumption of 2-(2-oxoacenaphthylen-1(2H)-ylidene)malononitrile monitored by TLC, the solvent was removed to afford crude product A (1-Oxo-1*H*-phenalene-2, 3-dicarbonitrile), which was purified by column chromatography on silica gel eluted with DCM/aether petrolei (1:50 to 1:5, v/v) to a yellow solid, Yield 84 %. ^{1}H NMR (400 MHz, DMSO-d6), *δ:* 8.72 (d, 1H, *J* = 7.2, 0.8 Hz), 8.67 (m, 1H, *J* = 8.0, 0.8 Hz), 8.64 (d, 1H, *J* = 7.2 Hz), 8.44 (t, 1H, *J* = 8.4 Hz), 8.07 (t, 1H, *J* = 8.0, 7.6 Hz) 7.98 (m, 1H, *J* = 7.8 Hz); ^{13}C NMR (100 MHz, DMSO-d6): *δ:* 174.5, 136.3, 136.0, 135.8, 134.8, 134.7, 132.2, 129.2, 126.3, 125.9, 119.3, 116.0, 112.5, 109.5, 107.3. HRMS: m/z calcd for $C_{15}H_6N_2O$: 230.0480, found: 230.0488.

The synthesis of OPD-A (4-((2,3-Dicyano-1-oxo-2,3-dihydro-1*H*-phenalen-6-yl)amino)butanoic acid)

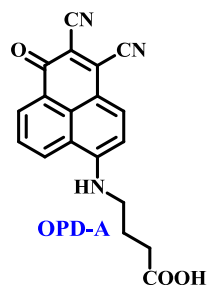

A (1.0 mmol) was suspended in anhydrous CH_3CN:CH_3OH (1:1) and stirred at room temperature for 5 min. 4-aminobutanoic acid (1.1 equiv) was then added in portions and the resultant solution was continued to stir at room temperature for 4.0 h. After removal of solvents by evaporation under reduced pressure, the crude products were purified by silica gel chromatography with DCM/MeOH (100:1 to 20:1, v/v) as eluent to a red solid (**OPD-A**), Yield 55 %. ^{1}H NMR (400 MHz, DMSO-d6), *δ:* 9.51 (s, 1H), 8.79 (d, 1H, *J* = 7.6, 0.6 Hz), 8.34 (d, 1H, *J* = 7.6, 0.6 Hz), 7.62 (t, 2H, *J* = 9.2 Hz), 7.41 (d, 1H, *J* = 7.8 Hz), 6.70 (d, 1H, *J* = 9.2 Hz), 3.64 (d, 2H), 3.20 (d, 2H, *J* = 6.7 Hz), 1.90 (s, 2H, *J* = 6.8 Hz); ^{13}C NMR (100 MHz, DMSO-d6): *δ:* 181.8, 174.5, 155.8, 139.3, 133.2, 132.4, 130.5, 128.6, 127.5, 126.1, 123.4, 116.6, 115.5, 112.5, 108.5, 105.5, 49.5, 42.4, 28.5. HRMS: m/z calcd for $C_{19}H_{13}N_3O_3$: 331.0857, found: 331.0851.

The synthesis of OPM ((((2*R*,3*S*,4*S*,5*R*)-5-(6-Amino-9*H*-purin-9-yl)-3,4-dihydroxytetrahydrofuran-2-yl)methyl)triphosphoric 4-((2,3-dicyano-1-oxo-1H-phenalen-6-yl)amino)butanoic anhydride)

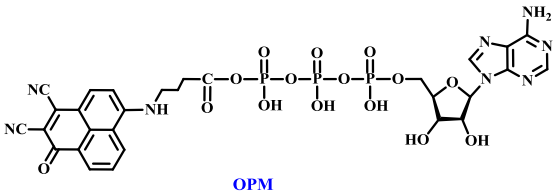

OPM

To **OPD-A** (1.0 mmol) in DMF (20 mL), EDCl (1.5 equiv), 1.0% DMAP. After 4.0 h, then, add ATPNa (1.0 equiv) into it. Reaction 16 h at room temperature. After removal of solvents by evaporation under reduced pressure, the crude products were purified by silica gel chromatography with DCM/MeOH (100:1 to 20:1, v/v) as eluent to a red solid (**OPM**). Yield 40 %. ^{1}H NMR (400 MHz, DMSO-d6), δ:10.67 (s, 3H), 8.83 (m, *J* = 8.30 Hz, 1H), 8.75 (m, 1H), 8.68 (m, *J* = 6.80 Hz, 1H), 8.53 (m, *J* = 8.50 Hz, 1H), 8.37 (d, 1H), 8.02(m, 1H), 7.88 (m, 1H), 7.65(d, 2H),7.01-6.96 (m, 1H), 6.10 (s, 1H), 4.48 (m, 3H), 3.94 (m, 2H), 3.62 (m, *J* = 5.90 Hz, 2H), 3.44 (m, 2H), 3.26 (m, *J* = 6.60 Hz, 2H), 1.62 (m, 2H, *J* = 6.8 Hz). ^{13}C NMR (600 MHz, DMSO-d6) *δ*: 181.8, 174.5, 155.8, 153.4, 150.1, 141.1, 140.5, 139.3, 133.2, 132.4, 130.5, 129.6, 128.5, 127.1, 125.4, 124.1, 119.6, 115.5, 116.5, 108.5, 105.5, 98.1, 86.5, 73.3, 70.5, 65.5, 49.5, 42.4, 28.5. HRMS: m/z calcd for $C_{29}H_{27}N_8O_{15}P_3$: 820.0809, found: 820.0815.

Abbreviations used in the text: ICT: intramolecular charge transfer; OPM: (((2R,5R)-5-(6-amino-9H-purin-9-yl)-3,4-dihydroxytetrahydrofuran-2-yl)methyl)triphosphoric 4-((2,3-dicyano-1-oxo-1Hphenalen-6-yl)amino)butanoic anhydride; and OPD: (4-((2,3-dicyano-1-oxo-1H-phenalen-6-yl)amino)butanoic phosphonic anhydride)

4. Monitor the response process of OPM for mitochondrial ATPase

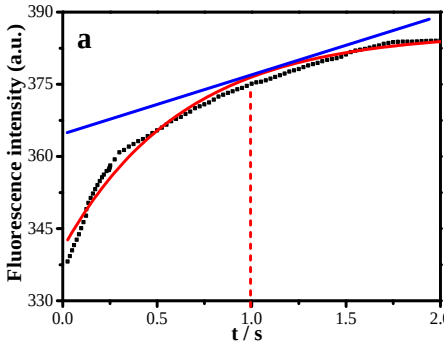

b.

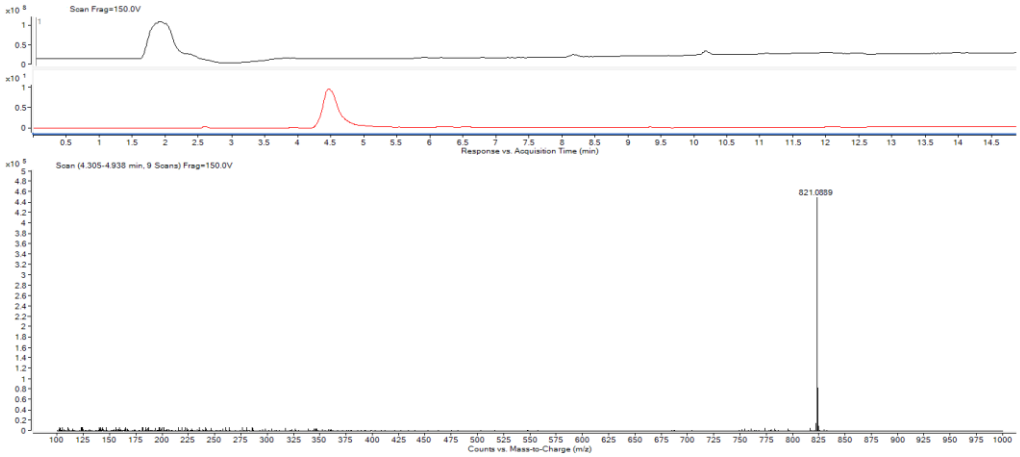

c.

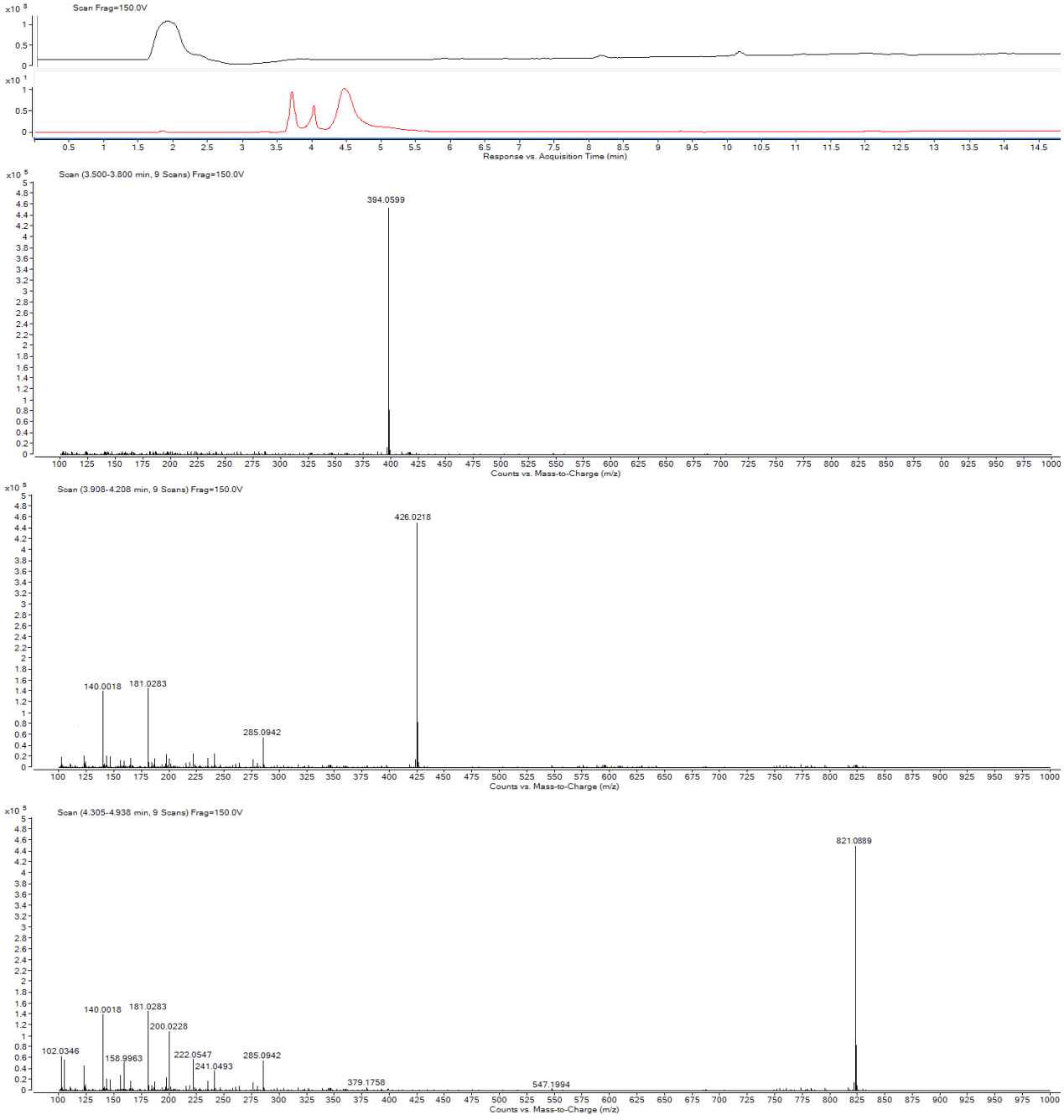

Figure S1. (a) The response time of **OPM** for mitochondrial ATPase. (b) and (c) Monitor the response process of **OPM** for mitochondrial ATPase by HRMS spectrum. (b) before; (c) after.

5. The optical testing of OPM and OPD^-

(1) The basic optical data of OPM and OPD^-.

Table S1. The basic optical data of OPM and OPD^-

	OPM	OPD^-
Fomula	$C_{29}H_{27}N_8O_{15}P_3$	$C_{19}H_{13}N_3O_5P^-$
λ_{ex}/nm	520	570
ε / M^{-1} cm^{-1}	1.2×10^5	2.2×10^5
λ_{em}/nm	565	590
Φ	0.78	0.75

(2) The reproducibility and selectivity of OPM for mitochondrial ATPase.

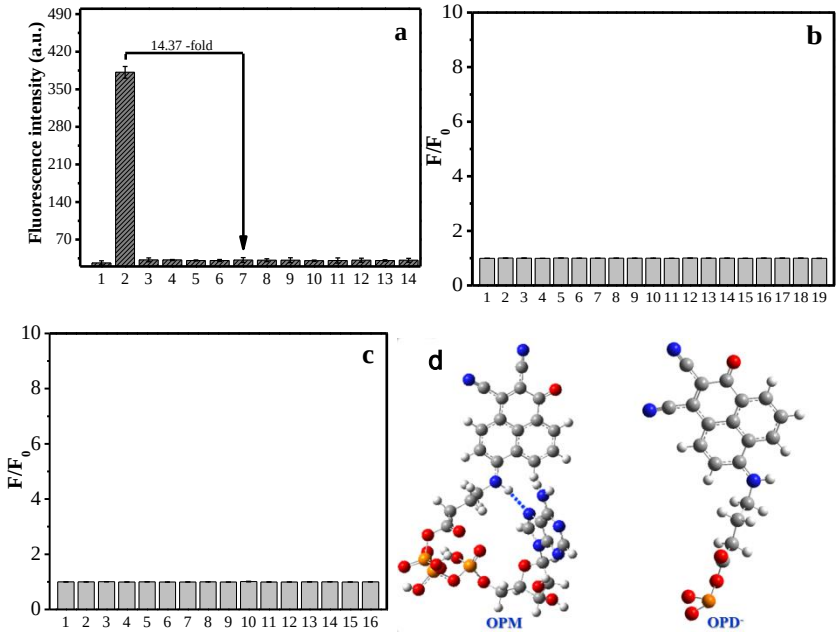

Figure S2. (a) Protein and enzyme interferent: 1, control; 2, ATPase; 3, RNA; 4, DNA; 5, triacylglycerol acylhydrolase; 6, lysozyme; 7, proteinase k; 8, histone; 9, collagen; 10, hemoglobin; 11, BSA; 12, β-amylase; 13, trypsin; and 14, chymotrypsin. (b) Amino acid interferent: 1, cystine; 2, DL-Threonine; 3, glutamic acid; 4, (S)-2-Amino-3-mercaptopropionic acid; 5, DL-Homocysteine; 6, Arginine; 7, glutamine; 8, glycine; 9, F-L-tyrosine; 10, F - DL – phenylalanine; 11, L-aspartic acid; 12, lysine; 13, serine; 14, DL-Leucine; 15, d-methionine; 16, d-methionine;17, hypoxanthine; 18, dithiothreitol; 19, trioxypurine. (c) Ion interferent: 1, NaCl; 2, $Pb(NO_3)_2$; 3, Na_2CO_3; 4, $CuSO_4$; 5, $Al(NO_3)_3$; 6, $MaSO_4$; 7, $NiCl_2{\cdot}6H_2O$; 8, Li_2CO_3; 9. KH_2PO_4; 10, K_2HPO_4; 11, $CrCl_3{\cdot}6H_2O$; 12, $ZnSO_4$; 13, $FeCl_3$; 14, $HgCl_2$; 15, $AgNO_3$; 16, $CaCl_2$.(d) The optimized conformation of OPM and OPD^- in water at the B3LYP/6-311G (d, p) level by Gaussian 09.

(3) The two-photon properties of OPM and OPD^{-}.

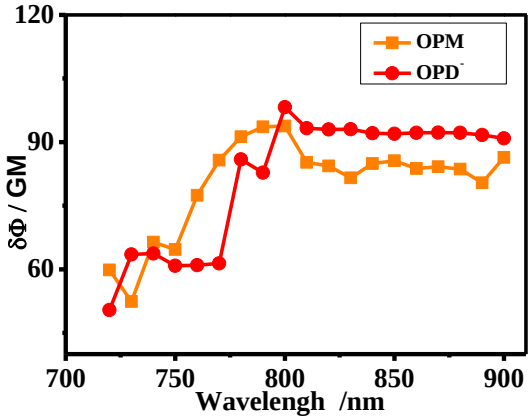

Figure S3. The two-photon properties of **OPM** and **OPD**$^{-}$.

(4) The photostability, pH-stability and water solubility of OPM and OPD^-.

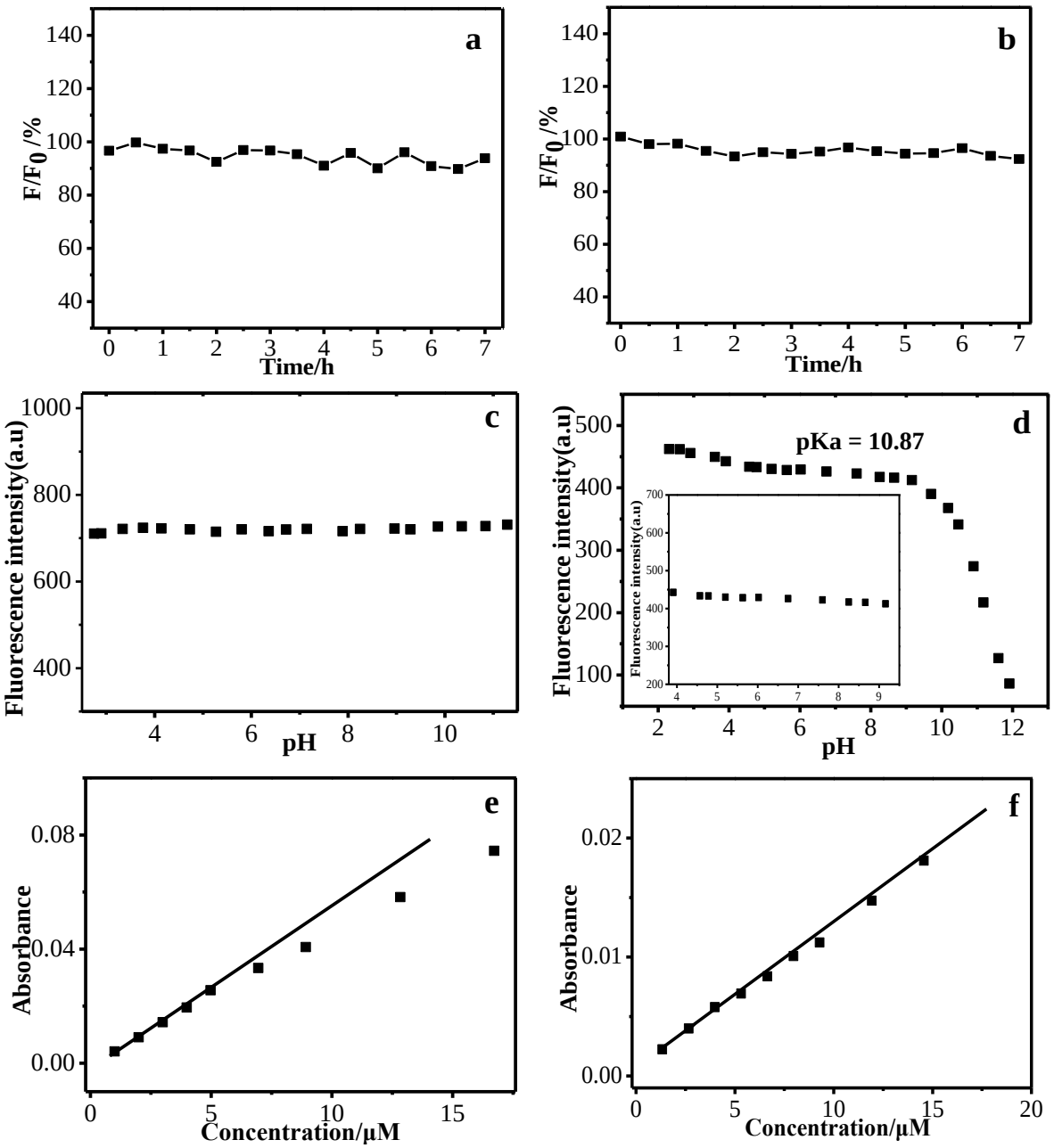

Figure S4. The photostability (a and b), pH-stability (c and d) and water solubility (e and f) of **OPM** (a, c and e) and **OPD^-** (b, d and f). Photostability, irradiation time: 7.0 h.

6. The cytotoxicity of OPM and OPD$^-$

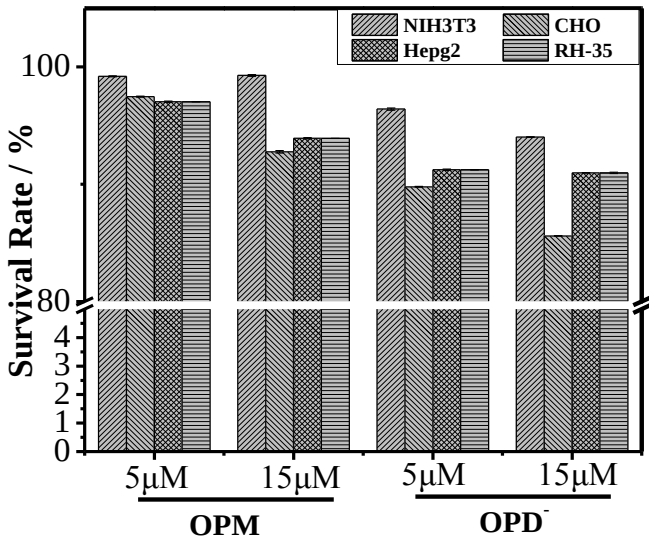

Figure S5. Cytotoxicity toxicity of **OPM** (5.0 μM and 15 μM) and **OPD**$^-$ (5.0 μM and 15 μM).

In order to real-time monitor mitochondrial ATPase activity in living organisms, the biological adaptability of **OPM** (such as cell viability and toxicity) must be verified. Because two-photon microscopy imaging technology possesses excellent biological adaptability, the activated two-photon action cross section $(\Phi\delta)_{max}$ of **OPM** and **OPD**$^-$ (4-((2,3-dicyano-1-oxo-1H-phenalen-6-yl)amino)butanoic phosphonic anhydride) were determined, firstly. And their values (Fig. S3) were 94 GM and 98 GM (1 GM = 10^{-50} cm^4 s/photon) at 800 nm, thereby suggesting that **OPM** and **OPD**$^-$ are favorable for the two-photon imaging in biological systems. Both the two species (**OPM** and **OPD**$^-$) showed high photostability (Fig. S4a and S4b), pH-stability (Fig. S4c and S4d) and appropriate water solubility in vitro (Fig.S4e and S4f), and were minimally cytotoxic to living cells, including cancer cell lines (Hepg 2 cell lines and RH35 cells lines) and non-cancer cell lines(CHO cell lines and NIH 3T3 cell lines), as assessed by MTT method (Fig. S5).

7. The cell imaging of OPM

(1) Two-photon imaging

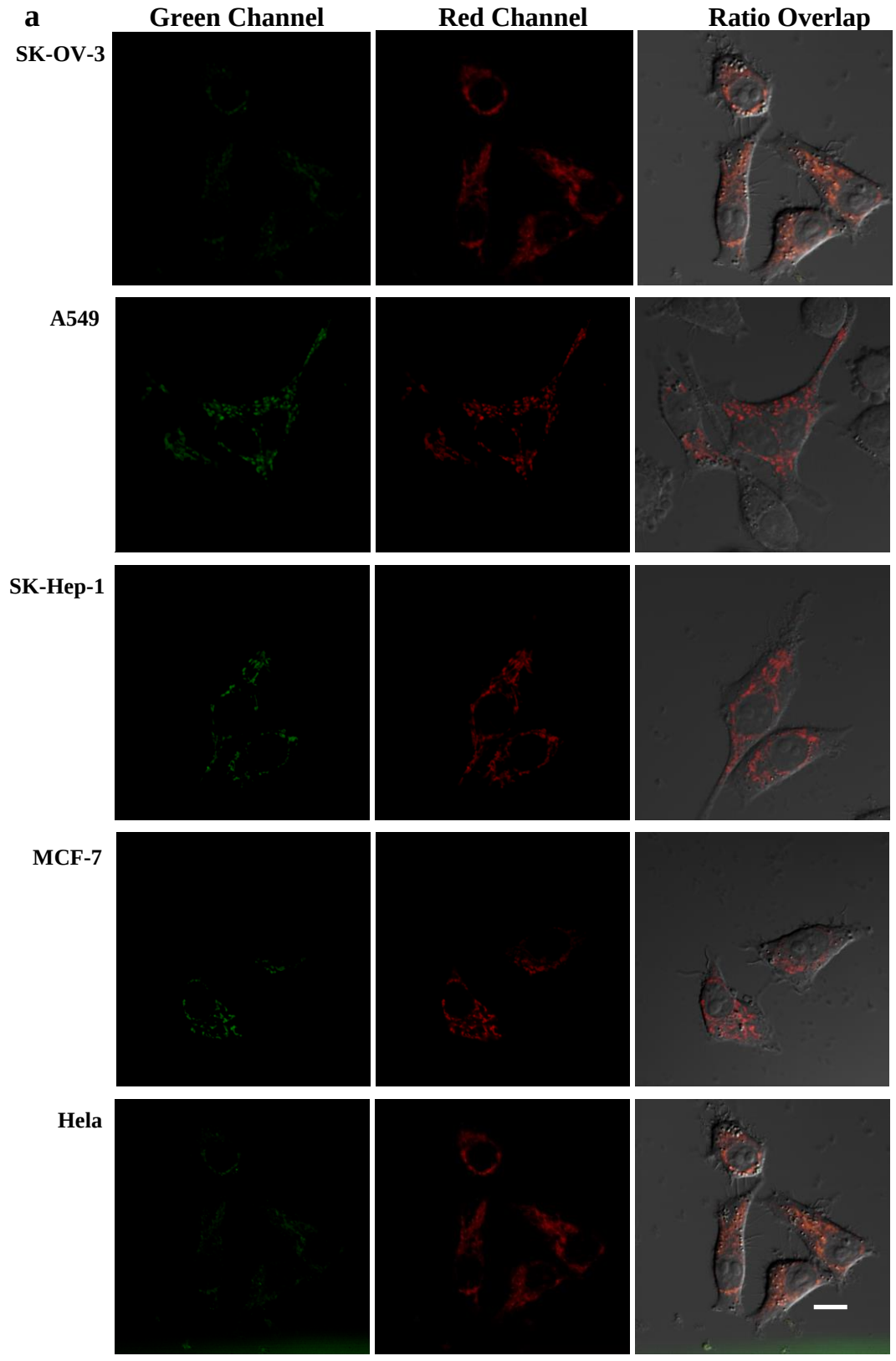

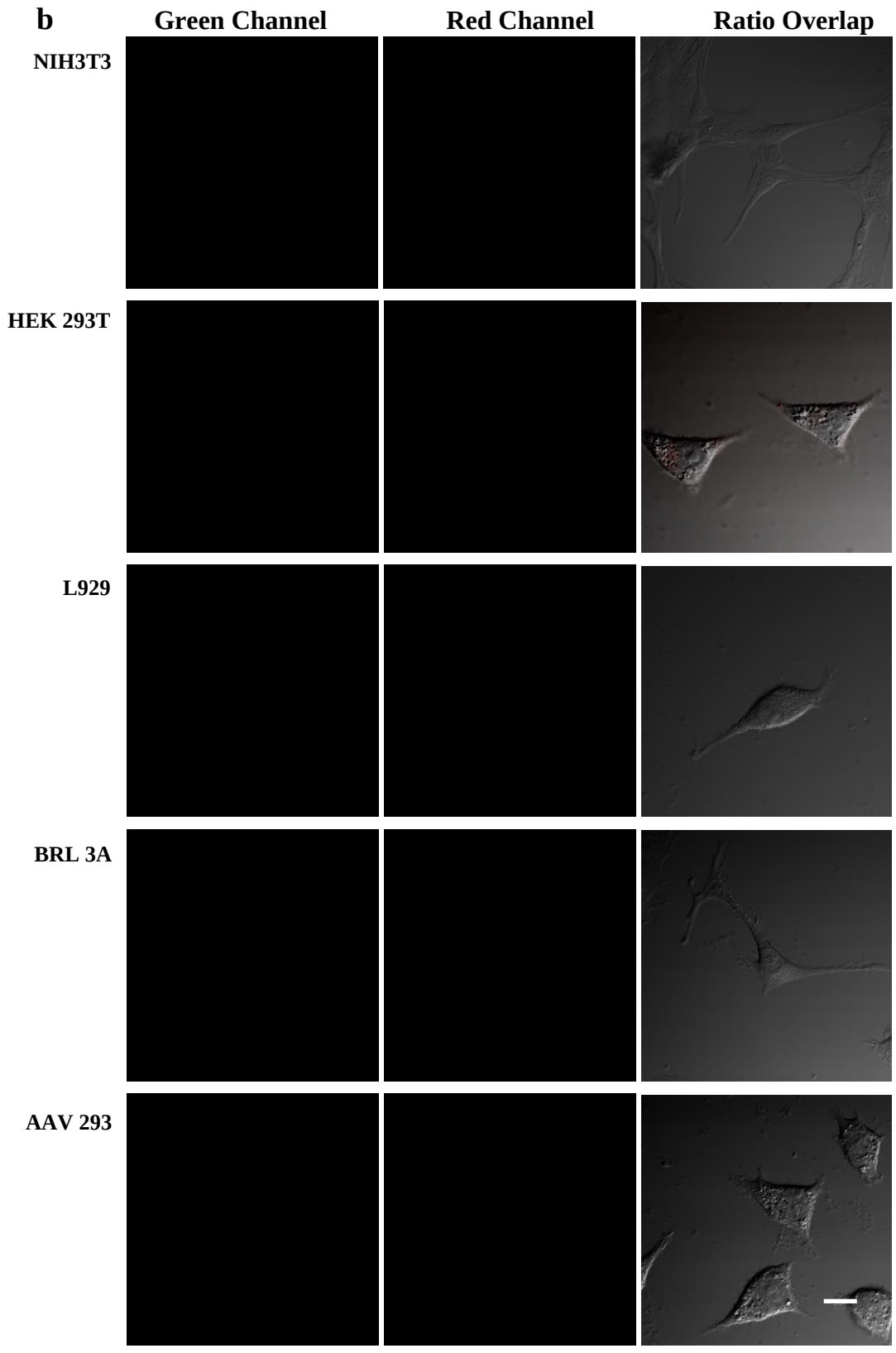

Figure S6. Cell imaging of **OPM** (5.0 μM), Green Channel: 555-575 nm, Red Channel: 580-600 nm, Excitation Wavelength: 800 nm. Ratio Overlap: Red channel/Green channel with Bright field imaging. Scale Represent: 20 μm.

(2) One-photon imaging

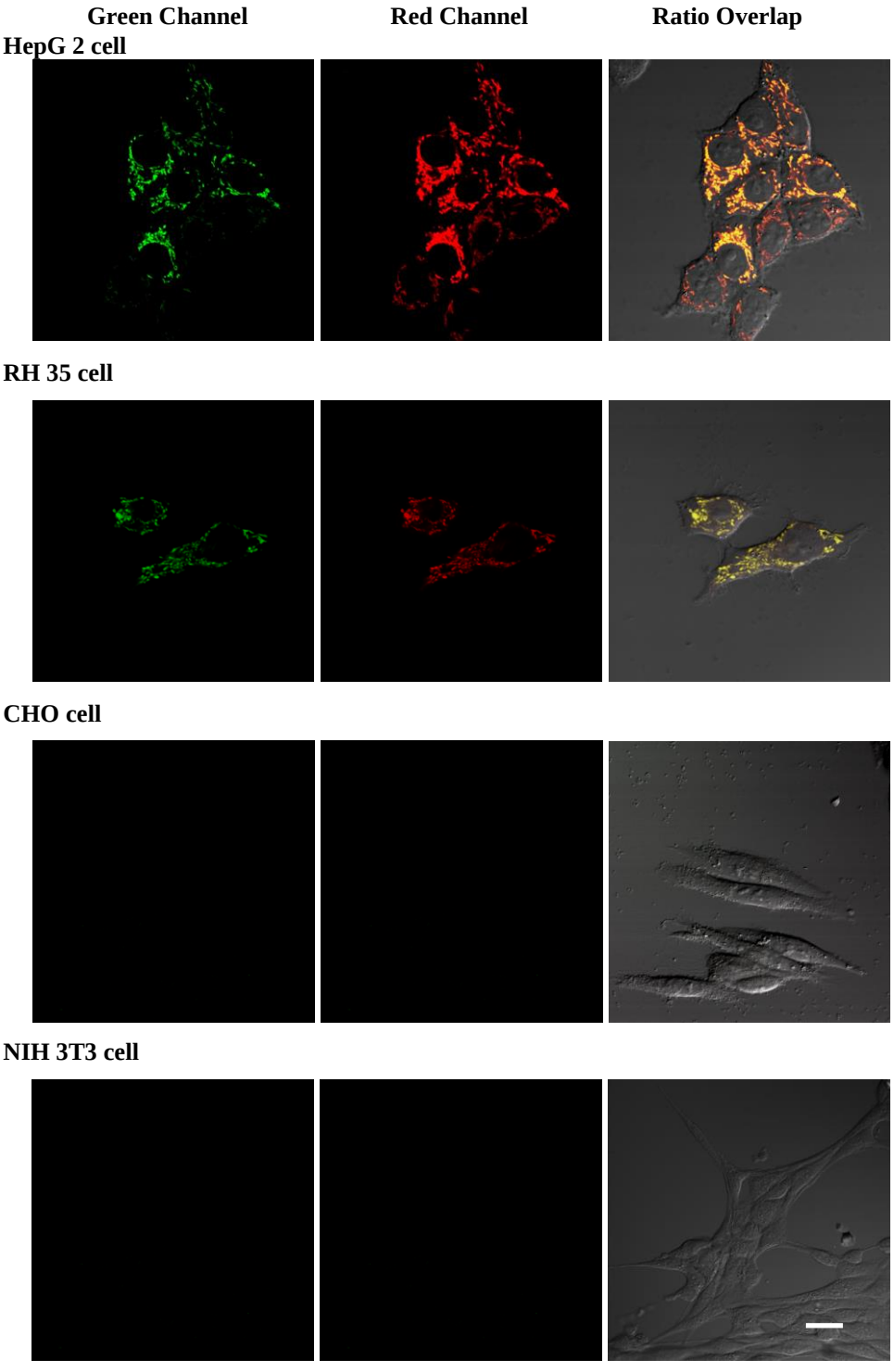

Figure S7. Cell imaging of **OPM** (5.0 μM), Green Channel: 555-575 nm, Red Channel: 580-600 nm, Excitation Wavelength: 559 nm and 515 nm. Ratio Overlap: Red channel/Green channel with Bright field imaging. Scale Represent: 15 μm.

8. The log P_{oct} values of **OPM** and **OPD$^-$**

Table S2. The log P_{oct} values of **OPM** and **OPD$^-$**

Probe species	log P_{oct}
OPM	0.3
OPD$^-$	-1.4
Species entering into cancer cells	> 0
Species accumulating in mitochondria	5 > log $P_{neutral\ species}$ > 0 0 > log P_{cation} > -5

Hydrophilicity-lipophilicity is modeled by the logarithm of the water-octanol partition coefficient (log P_{oct}). Probes specifically entering cancer cells are assigned numerically by the following criteria: log $P_{neutral\ species}$ > 0.[28,29] log P_{oct} values (Table S2) of OPM is 0.3, thereby suggesting its easy membrane permeability for cancer cells. Furthermore, if probe specifically accumulates in the mitochondria, its log P_{oct} values must be 5 > log $P_{neutral\ species}$ > 0; 0 > log P_{cation} > -5.[28,29] In our case, log P_{oct} values of OPM (0.3) and its metabolite OPD$^-$ (-1.4) reach the above criteria. These estimated results indicate that the both OPM and OPD$^-$ mainly accumulate in mitochondria of cancer cells.

9. Quantum Calculation Data

The structure optimization of OPD-Mito

Symbolic Z-matrix: Charge = 0, Multiplicity = 1

C	-5.07008	-2.05851	-0.86993
O	-4.88503	-1.01783	-1.86607
P	-3.97702	0.24803	-1.58946
O	-5.08824	1.28219	-0.84888
P	-4.70182	2.82611	-0.69627
O	-4.18461	2.90869	0.86045
P	-3.80931	4.36125	1.51919
O	-2.26835	4.53741	0.99481
C	-4.56081	-3.37006	-1.45393
C	-4.84846	-4.5942	-0.57677
C	-3.62663	-4.62495	0.36043
C	-2.51393	-4.15462	-0.61657
O	-3.12807	-3.33257	-1.59222
O	-3.88144	-3.74213	1.42168
O	-4.88078	-5.71705	-1.44583
O	-3.71752	4.0728	3.06864
O	-6.10902	3.55761	-0.67505
O	-3.84791	0.84313	-3.05956
O	-4.7272	5.41822	1.05708
O	-3.67649	3.26037	-1.68185
O	-2.75977	0.10339	-0.76301
N	-1.41412	-3.39353	-0.00276
C	-0.85318	-3.50931	1.25594
C	0.30527	-2.72744	1.22451
N	-1.31553	-4.19172	2.31717
C	-0.51531	-4.06614	3.38457
N	0.63017	-3.38866	3.48423
C	1.07175	-2.69992	2.41223

N	2.22027	-1.99598	2.54322
N	0.45465	-2.13116	-0.01931
C	-0.58089	-2.5551	-0.70946
C	6.16354	-2.46451	-0.35682
C	4.80856	-2.77771	-0.49681
C	3.87019	-1.76496	-0.64939
C	4.25189	-0.40475	-0.65681
C	5.64308	-0.08728	-0.54786
C	6.5858	-1.13941	-0.38813
C	3.283	0.67575	-0.78978
C	3.76897	1.99446	-0.88019
C	5.12566	2.27427	-0.79477
C	6.08353	1.27009	-0.61241
C	8.04142	-0.86018	-0.25554
C	7.49045	1.55528	-0.49742
C	8.43716	0.56144	-0.32473
O	8.86732	-1.75659	-0.0981
N	1.95539	0.40239	-0.83369
C	-0.5071	3.19923	0.09242
C	0.536	2.10612	0.34447
C	0.90514	1.40021	-0.97383
C	-1.33325	3.54412	1.29282
O	-1.2949	3.03322	2.38876
C	9.82619	0.86136	-0.20599
N	10.9596	1.10644	-0.10795
C	7.90642	2.92817	-0.56409
N	8.19806	4.05253	-0.62198
H	-4.54145	-1.81752	0.0536
H	-6.1459	-2.10684	-0.67995
H	-4.98131	-3.51407	-2.45348
H	-5.77063	-4.49521	0.0098
H	-3.41364	-5.64174	0.71654
H	-2.07638	-5.02413	-1.12267
H	-3.15669	-3.88739	2.07142
H	-5.08854	-6.50245	-0.91553
H	-2.86965	3.60603	3.27477
H	-6.02463	4.43365	-0.22968
H	-3.59811	1.79506	-2.99691
H	-0.83873	-4.5848	4.28394
H	2.75464	-2.14882	3.38754
H	2.71704	-1.67037	1.72617
H	-0.81105	-2.28054	-1.72802
H	6.91692	-3.23634	-0.23532
H	4.4864	-3.81491	-0.49933
H	2.8299	-2.04299	-0.7866
H	3.0768	2.8189	-0.99608
H	5.44995	3.30897	-0.85705
H	1.6168	-0.53217	-0.60098
H	-0.06984	4.12488	-0.30369
H	-1.24203	2.88423	-0.66368
H	0.12996	1.36291	1.03729
H	1.42804	2.53027	0.81817
H	1.19752	2.12644	-1.74131
H	0.01709	0.88015	-1.3474

Standard orientation:

Center Number	Atomic Number	Atomic Type	Coordinates (Angstroms) X	Y	Z
1	6	0	5.070076	2.058506	-0.869925
2	8	0	4.885032	1.017830	-1.866067
3	15	0	3.977022	-0.248028	-1.589455
4	8	0	5.088235	-1.282189	-0.848878
5	15	0	4.701822	-2.826113	-0.696273
6	8	0	4.184607	-2.908689	0.860448
7	15	0	3.809313	-4.361255	1.519194
8	8	0	2.268350	-4.537412	0.994807
9	6	0	4.560805	3.370058	-1.453927
10	6	0	4.848464	4.594198	-0.576773
11	6	0	3.626629	4.624952	0.360431
12	6	0	2.513928	4.154621	-0.616570
13	8	0	3.128067	3.332565	-1.592223
14	8	0	3.881443	3.742125	1.421683
15	8	0	4.880781	5.717047	-1.445834
16	8	0	3.717524	-4.072800	3.068640
17	8	0	6.109016	-3.557609	-0.675048
18	8	0	3.847914	-0.843127	-3.059561
19	8	0	4.727196	-5.418224	1.057081
20	8	0	3.676485	-3.260371	-1.681847
21	8	0	2.759773	-0.103394	-0.763008
22	7	0	1.414121	3.393528	-0.002760
23	6	0	0.853179	3.509308	1.255935
24	6	0	-0.305272	2.727436	1.224508
25	7	0	1.315527	4.191721	2.317174
26	6	0	0.515312	4.066138	3.384574
27	7	0	-0.630171	3.388656	3.484231
28	6	0	-1.071750	2.699917	2.412233
29	7	0	-2.220270	1.995980	2.543216
30	7	0	-0.454649	2.131163	-0.019306
31	6	0	0.580892	2.555104	-0.709455
32	6	0	-6.163536	2.464512	-0.356824
33	6	0	-4.808564	2.777705	-0.496808
34	6	0	-3.870188	1.764960	-0.649392
35	6	0	-4.251892	0.404749	-0.656809
36	6	0	-5.643078	0.087283	-0.547855
37	6	0	-6.585801	1.139407	-0.388128
38	6	0	-3.283004	-0.675753	-0.789775
39	6	0	-3.768967	-1.994460	-0.880187
40	6	0	-5.125664	-2.274268	-0.794770
41	6	0	-6.083528	-1.270085	-0.612410
42	6	0	-8.041422	0.860182	-0.255544
43	6	0	-7.490447	-1.555276	-0.497415
44	6	0	-8.437162	-0.561441	-0.324725
45	8	0	-8.867323	1.756587	-0.098100

46	7	0	-1.955391	-0.402388	-0.833692
47	6	0	0.507096	-3.199234	0.092424
48	6	0	-0.535996	-2.106118	0.344472
49	6	0	-0.905144	-1.400207	-0.973827
50	6	0	1.333247	-3.544118	1.292822
51	8	0	1.294897	-3.033215	2.388756
52	6	0	-9.826186	-0.861359	-0.205990
53	7	0	-10.959599	-1.106438	-0.107953
54	6	0	-7.906419	-2.928167	-0.564093
55	7	0	-8.198063	-4.052525	-0.621984
56	1	0	4.541451	1.817523	0.053603
57	1	0	6.145895	2.106836	-0.679953
58	1	0	4.981312	3.514071	-2.453479
59	1	0	5.770629	4.495208	0.009803
60	1	0	3.413640	5.641737	0.716544
61	1	0	2.076379	5.024127	-1.122672
62	1	0	3.156691	3.887386	2.071417
63	1	0	5.088536	6.502454	-0.915531
64	1	0	2.869650	-3.606026	3.274768
65	1	0	6.024634	-4.433649	-0.229678
66	1	0	3.598114	-1.795058	-2.996909
67	1	0	0.838733	4.584795	4.283943
68	1	0	-2.754640	2.148824	3.387537
69	1	0	-2.717042	1.670365	1.726165
70	1	0	0.811048	2.280538	-1.728016
71	1	0	-6.916915	3.236337	-0.235320
72	1	0	-4.486402	3.814906	-0.499333
73	1	0	-2.829902	2.042992	-0.786602
74	1	0	-3.076802	-2.818896	-0.996080
75	1	0	-5.449951	-3.308968	-0.857051
76	1	0	-1.616801	0.532169	-0.600975
77	1	0	0.069838	-4.124885	-0.303688
78	1	0	1.242025	-2.884233	-0.663683
79	1	0	-0.129961	-1.362913	1.037286
80	1	0	-1.428037	-2.530265	0.818168
81	1	0	-1.197517	-2.126440	-1.741305
82	1	0	-0.017090	-0.880148	-1.347399

References

S1. Li, H.; Liu, F.; Xiao, Y.; Pellechia, P. J.; Smith, M. D.; Qian, X.; Wang, G.; Wang, Q. *Tetrahedron*, **2014**, *70*, 5872-5877.

Attached Spectra

(1) ^{1}H NMR

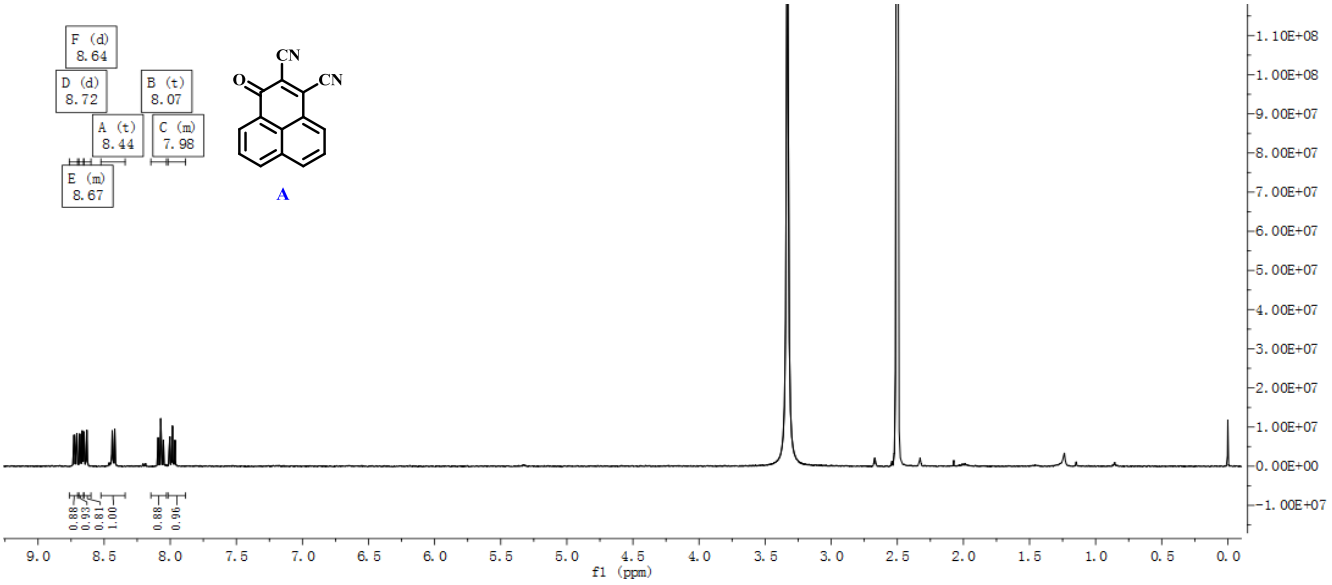

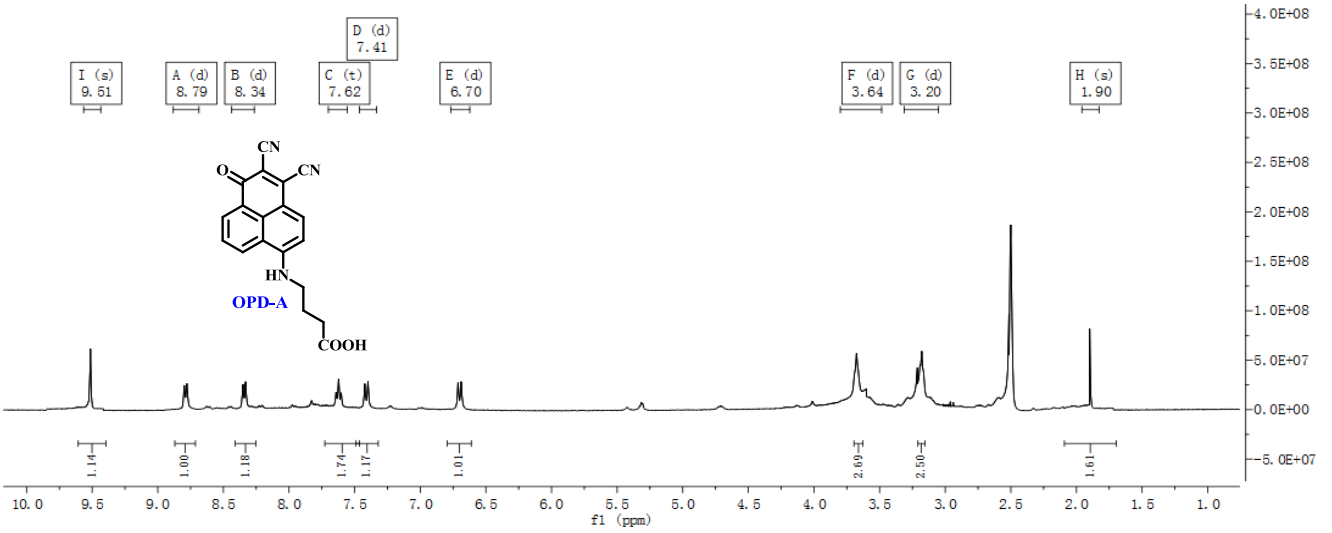

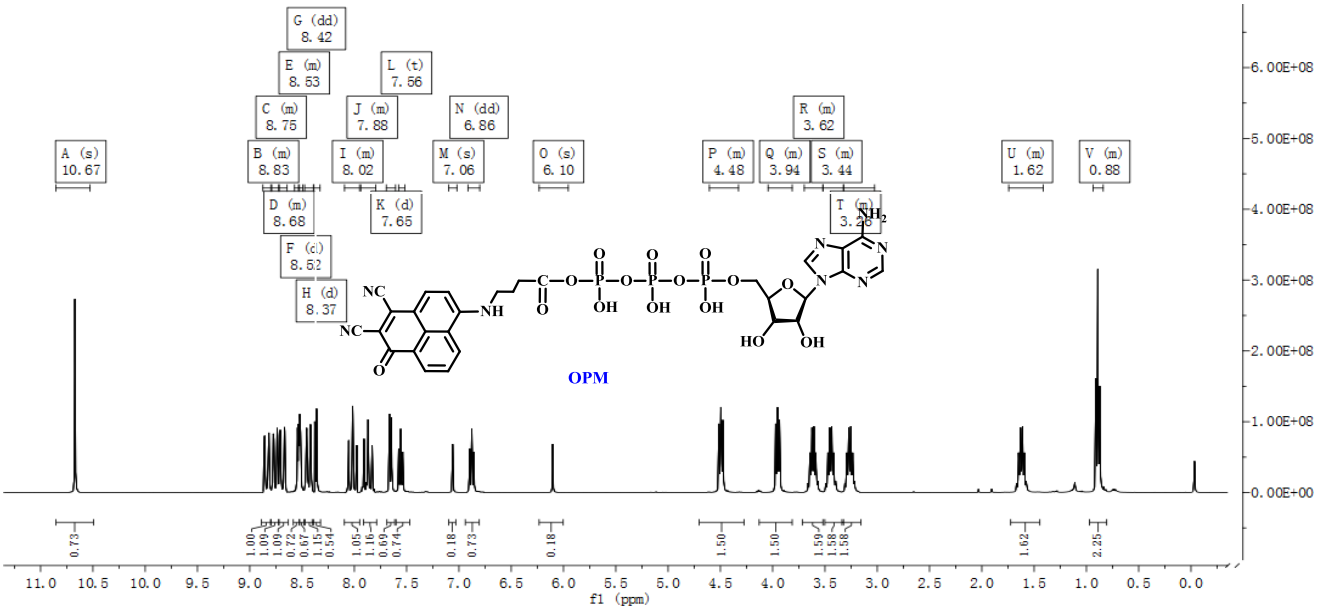
A (s) 10.67
G (dd) 8.42
E (m) 8.53
L (t) 7.56
C (m) 8.75
J (m) 7.88
N (dd) 6.86
B (m) 8.83
I (m) 8.02
M (s) 7.06
O (s) 6.10
D (m) 8.68
K (d) 7.65
F (d) 8.52
H (d) 8.37
P (m) 4.48
Q (m) 3.94
S (m) 3.44
R (m) 3.62
T (m) 3.28
U (m) 1.62
V (m) 0.88
OPM
f1 (ppm)

(2) ^{13}C NMR

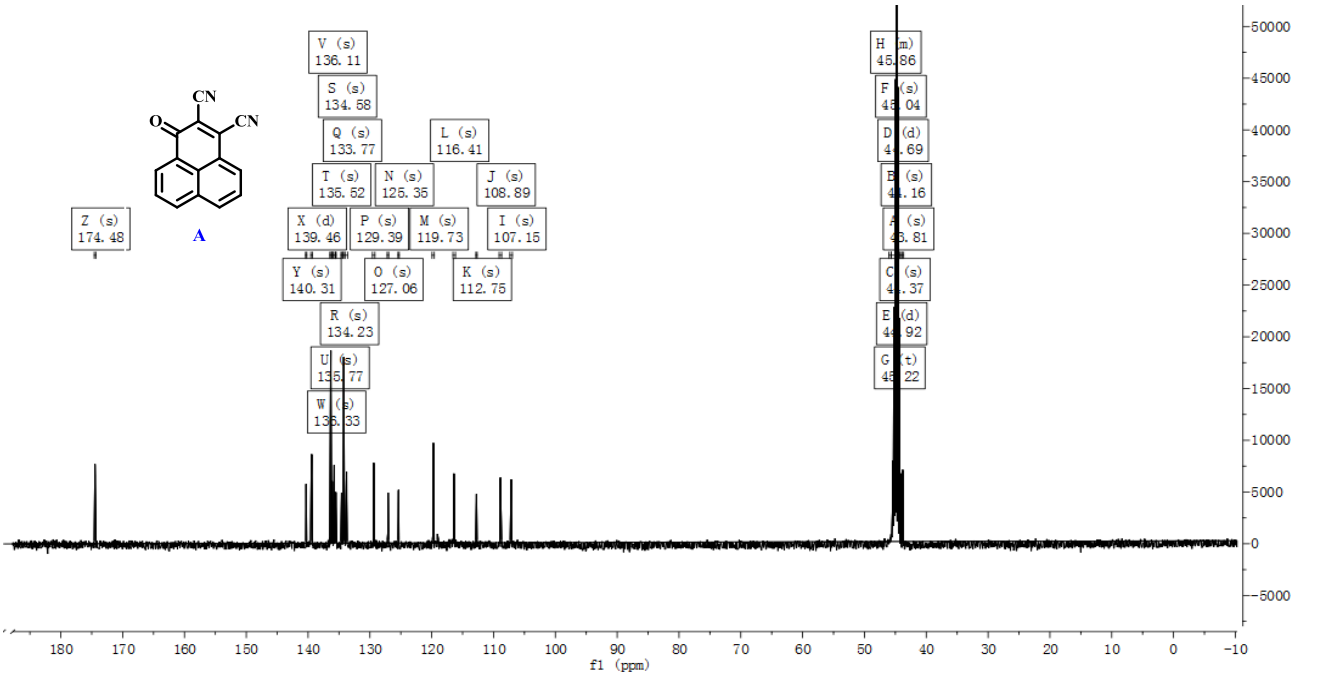
A
Z (s) 174.48
V (s) 136.11
S (s) 134.58
Q (s) 133.77
L (s) 116.41
T (s) 135.52
N (s) 125.35
J (s) 108.89
X (d) 139.46
P (s) 129.39
M (s) 119.73
I (s) 107.15
Y (s) 140.31
O (s) 127.06
K (s) 112.75
R (s) 134.23
U (s) 135.77
W (s) 135.33
H (m) 45.86
F (s) 45.04
D (d) 44.69
B (s) 44.16
A (s) 43.81
C (s) 44.37
E (d) 44.92
G (t) 43.22
f1 (ppm)

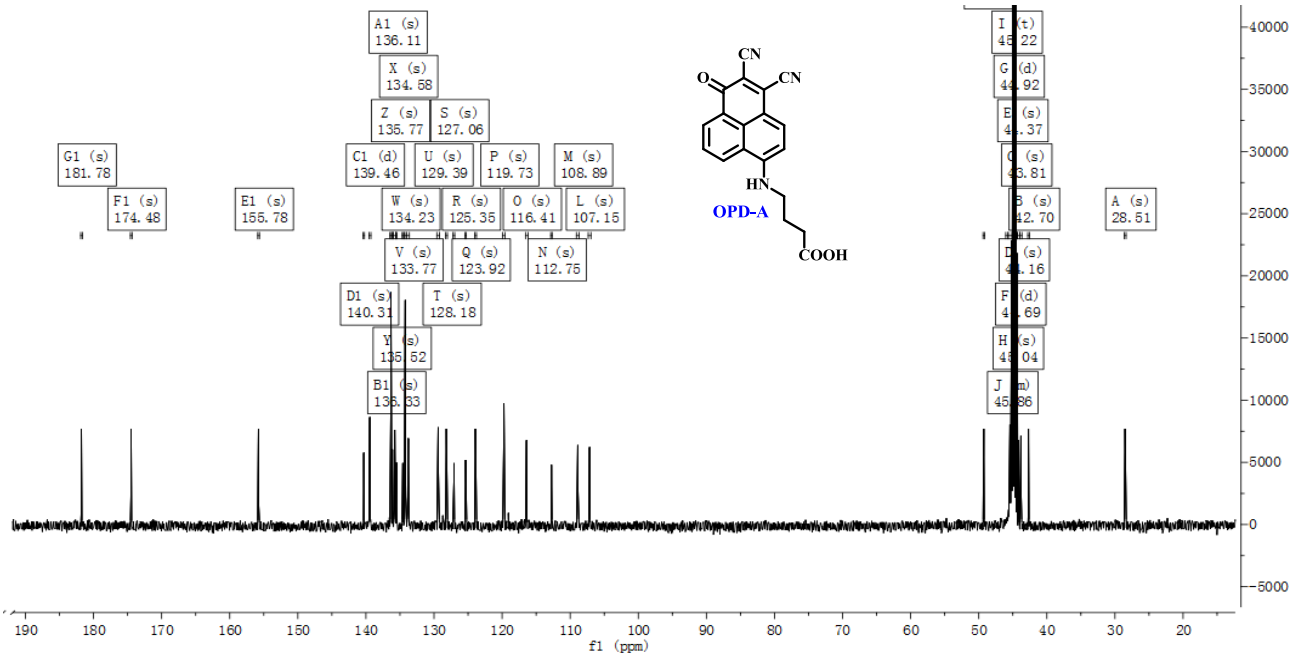
OPD-A
CN
CN
O
HN
COOH
f1 (ppm)

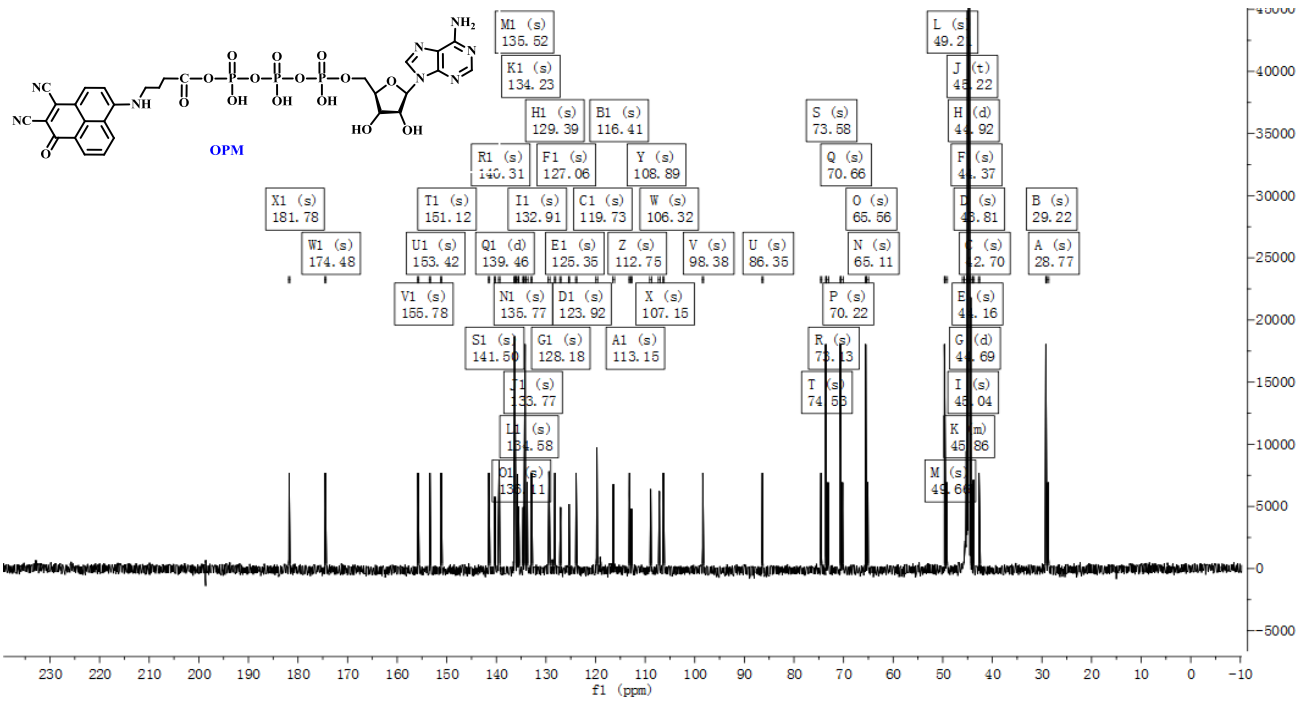
OPM
NC
NC
NH
NH2
HO
OH
f1 (ppm)

Supporting Information-Video S1

The dynamic change of mitochondrial ATPase in cancer cells was observed on time-scan mode by Olympus spectral confocal multiphoton microscope (FV1200) with MaiTai femtosecond laser source (Spectra-Physics).

Supporting Information-Video S2

The dynamic change of mitochondrial ATPase in cancer cells apoptosis was observed on time-scan mode by Olympus spectral confocal multiphoton microscope (FV1200) with MaiTai femtosecond laser source (Spectra-Physics). Inverted microscope was used in cell imaging.